Journal on Electronic and Automation Engineering
Vol: 4(2), June 2025
REST Publisher; ISSN: 2583-6951 (Online)
Website: https://restpublisher.com/journals/jeae/
DOI: https://doi.org/10.46632/jeae/4/2/60

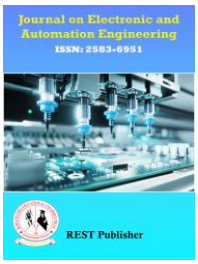

Distributed Energy Resources Based EV Charging Station with Seamless Connection to Grid

* P. Madhavi, K. Sowjanya, N. Madhukar Reddy
Siddhartha Institute of Technology and Sciences, Korremula, Hyderabad, Telangana, India.
**Corresponding author: madhavipasham2013@gmail.com*

Abstract: *The charging of electric vehicles (EVs) via common DC bus charging infrastructure based on hybrid renewable energy sources such as solar photovoltaic (PV) and fuel cell is presented here. The requisite to incorporate renewable energy based distributed energy resources (DERs) is attributed to the escalating concern for decarbonization with improved power quality requirements. Furthermore, the bidirectional flow of power enables the charging/discharging of EVs during the grid presence/absence modes of operation. In addition, the utilization of common DC bus charging mechanism for EVs facilitates fast charging capability at higher voltage levels. The satisfactory operation during the grid availability/unavailability is attained through the current and voltage-based control mechanisms, along with the seamless transition capability via switching (STS-1/0) of the static transfer switches. Furthermore, in compliance with the IEEE standards, the power quality (PQ) improvement is obtained with the utilization of an adaptive comb-filter based current control during the grid-tied mode of operation. The need for improving PQ stems from the fact that an uninterrupted supply is essential to the critical loads along with an improved power quality. Thus, for validation and corroboration of the system behavior, its performance is authenticated during weak grid conditions, in conjunction with grid connected/islanded modes of operation.*

Keywords: *Adaptive comb-filter, distribution network, EV charging, fuel cell stack, grid connected mode, islanded mode, power quality, seamless power transfer, solar PV array.*

1. INTRODUCTION

The rapid rise in electric vehicle (EV) adoption is driven by the global push for greener alternatives to fossil fuels, with the European Commission forecasting a tenfold increase in EV numbers. To meet this demand, hybrid renewable energy sources such as solar photovoltaic (PV) arrays, fuel cell stacks, and batteries are increasingly being deployed due to their environmental, technical, and economic benefits [1]. Rooftop PV arrays, in particular, are gaining traction for their ability to serve local loads, improve grid performance, and reduce feeder stress, while government subsidies further encourage adoption [2] [3]. However, the intermittent nature of solar power necessitates energy storage solutions to ensure reliability, with batteries offering uninterrupted supply to critical loads. Fuel cells, known for high efficiency and low emissions, are also emerging as essential components in hybrid distributed energy systems, complementing the variability of other sources [4] [5]. EVs, as flexible loads, can enhance microgrid resilience, provide frequency regulation, and serve as additional storage capacity, but renewable charging is essential to fulfill their environmental promise [6] [7]. To address the variability of solar insolation, charging stations are designed for both grid-connected and islanded modes with seamless switching, maximizing PV utilization and minimizing fluctuation impacts. Beyond EV charging, these stations support vehicle-to-home and vehicle-to-grid applications, improving power quality and reducing harmonic distortion in smart grids [8] [9]. However, challenges remain, including unused PV capacity during grid disconnection, battery overcharging risks, long charging times, and limited driving range. Integrating fuel cells with batteries is proposed as a viable solution for future plug-in hybrid configurations. This hybrid approach combining solar PV, fuel cells, and batteries requires advanced control algorithms to comply with IEEE standards and improve power quality [10]. Existing methods like second-order generalized integrators (SOGI), model predictive control, and least mean fourth (LMF) algorithms face limitations in dynamic performance, computational complexity, or convergence speed [11] [12]. To overcome these drawbacks, an

adaptive comb filter [13] is proposed for EV charging systems, offering fast convergence, low complexity, and synchronization capabilities. In grid-connected mode, it ensures harmonic mitigation per IEEE-519 [15], while in islanded mode, local loads are powered by PV and fuel cells to maintain service continuity. The system employs a common DC bus infrastructure for fast charging by bypassing onboard chargers, delivering high power directly to EV batteries through modular stacked converters. To avoid bulky onboard equipment, these converters are placed in charging stations with integrated AC/DC and DC/DC stages, including galvanic isolation for safety. The AC/DC stage performs power factor correction to maintain a stable DC link from AC input, while the DC/DC stage steps down voltage for battery charging, enabling reduced charging times and improved operational efficiency.

2. LITERATURE REVIEW

M. T. Lawder, in Battery Energy Storage System (BESS) and Battery Management System (BMS) for Grid-Scale Applications, identifies inefficiencies in the current electric grid arising from mismatches between power generation and consumption, leading to wasted electricity. BESS can address these inefficiencies, but effective deployment requires advanced modeling for accurate monitoring and control, managed by a robust BMS. The paper emphasizes that physics-based models enhance BMS performance for both lithium-ion and vanadium redox-flow batteries, discusses system architecture for improved monitoring, and outlines a development pathway for grid-scale applications. Similarly, Y. Zhang, N. Gatsis, and G. B. Giannakis, in Robust Energy Management for Microgrids with High-Penetration Renewables, propose a distributed economic dispatch framework for microgrids with high renewable penetration, operating in grid-connected mode. Their method addresses renewable energy variability by jointly considering actual renewable output and energy traded with the main grid, minimizing net costs including distributed generation, storage, load utility, and worst-case transaction costs through a dual decomposition approach that enables decentralized optimization. G. He, Q. Chen, C. Kang, and Q. Xia, in Optimal Offering Strategy for Concentrating Solar Power Plants in Joint Energy, Reserve and Regulation Markets, develop a robust and stochastic optimization framework to determine CSP plants' optimal day-ahead offering strategies, balancing ancillary services provision with solar energy accommodation to avoid excessive curtailment and revenue loss. The study introduces the maximum acceptable curtailment rate to quantify this trade-off, with case studies validating the model. P. Shukl and B. Singh, in Grid integration of three-phase single-stage PV system using adaptive laguerre filter based control algorithm under non-ideal distribution system, present a single-stage, three-phase PV system using MPPT (P&O technique) and an adaptive Laguerre filter for VSC control, supported by a PI controller for DC link voltage regulation. The system demonstrates robust performance under varying load and non-ideal conditions. Additionally, B. Singh, Chandra, and K. Al-Hadad, in Power Quality: Problems and Mitigation Techniques, highlight the increasing challenge of maintaining power quality due to widespread use of power electronics converters, noting associated issues such as increased losses, equipment malfunctions, and network disturbances, and emphasize the need for improved mitigation strategies.

3. PROPOSED METHODOLOGY

A Maximum Power Point Tracker (MPPT) is a high-efficiency DC–DC converter that optimizes the electrical load on a solar panel or array to operate at its maximum power point (MPP), where current (I) and voltage (V) produce peak output, corresponding to a load resistance equal to V/I and satisfying the condition $V/I = -dV/dI$. MPPT systems use control logic to continuously locate this point for maximum energy extraction. Traditional solar inverters perform MPPT on an entire array, causing energy losses when panel MPPs differ due to shading, soiling, or manufacturing variations, as the same current flows through all panels. To address this, some designs integrate power optimizers into individual panels, enabling each to operate at peak efficiency despite mismatches. In off-grid systems, MPPT is particularly valuable during battery charging, as the battery voltage especially when partially discharged at sunrise often differs from the PV array's MPP, and MPPT resolves this mismatch for optimal charging.

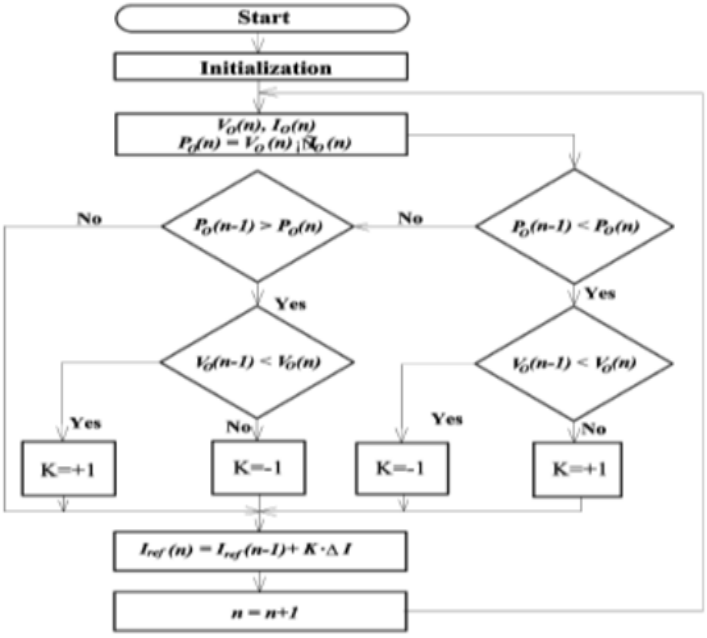

FIGURE 1. Flowchart of the MPPT algorithm with P&O method.

By comparing the recent values of power and voltage with previous ones, the P&O method shown in the flow chart can determine the value of reference current to adjust the output power toward the maximum point [4]. MPPTs can be designed to drive an electric motor without a storage battery. They provide significant advantages, especially when starting a motor under load. This can require a starting current that is well above the short-circuit rating of the PV panel. A MPPT can step the panel's relatively high voltage and low current down to the low voltage and high current needed to start the motor. Once the motor is running and its current requirements have dropped, the MPPT will automatically increase the voltage to normal. In this application, the MPPT can be seen as an electrical analogue to the transmission in a car; the low gears provide extra torque to the wheels until the car is up to speed.

A. Motivation

Owing to research gaps, the gaps observed provide the incentive for carrying out this work as follows. Renewable energy integration with improved power quality: Several power quality issues are observed with the integration of renewable energy based distributed energy resources (DERs). These PQ issues are eliminated in accordance with IEEE standards, through the usage of adaptive comb-filter during the grid-tied mode of operation along with the charging of EVs. Prevalent control techniques: The control techniques widely utilized have not reported efficient operation during weak grid conditions along with synchronization capability for charging of EVs, whereas, with the adaptive comb-filter, satisfactory performance is obtained along with the grid integration/disconnection ability.

B. Proposed Work

The adaptive comb-filter is utilized for the power quality improvement during grid interconnection along with the charging of EVs. The seamless transition between the grid connected and disconnected mode of operation is achieved for common DC bus EVs charging system. The usage of hybrid distributed energy sources such as solar PV array, battery and fuel cell stack, complements the variability of each other, thereby ensuring reliable and uninterrupted operation

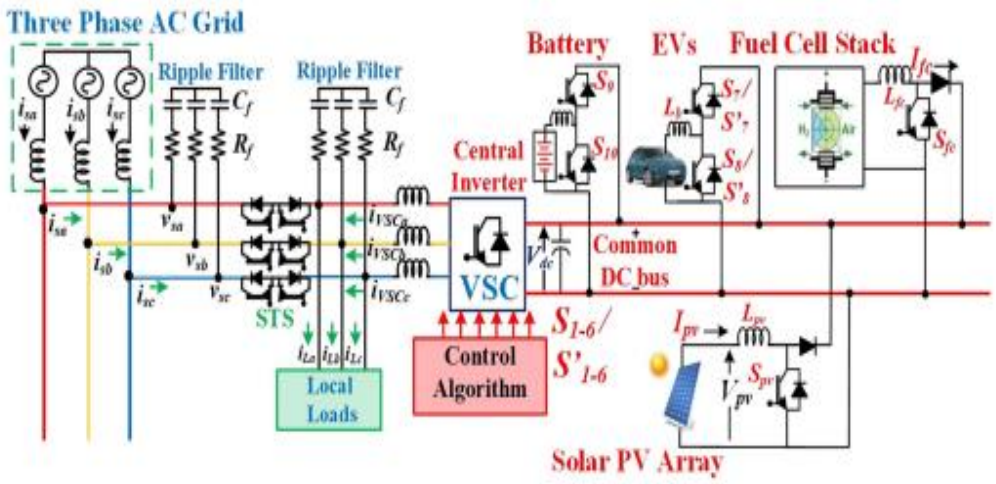

FIGURE 2. EVs charging system configuration with hybrid renewable energy sources

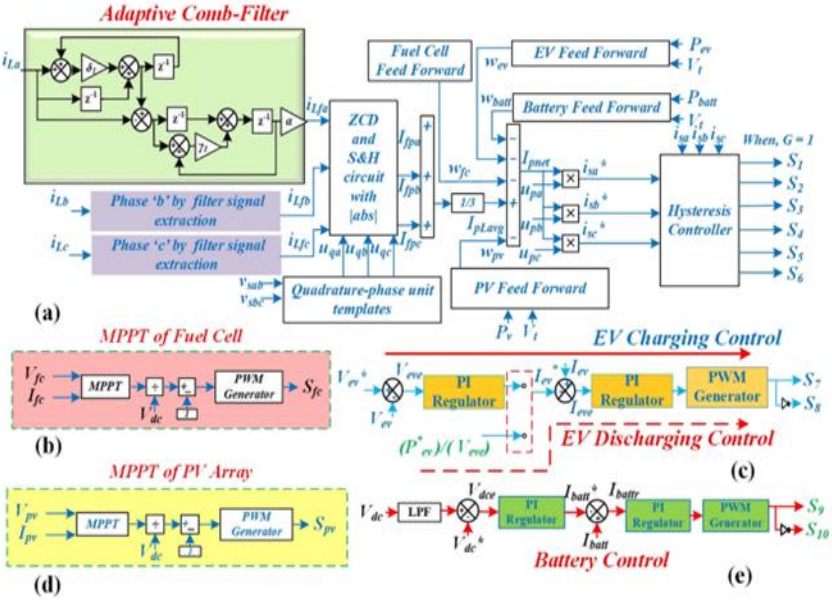

FIGURE 3. Control technique utilized during grid presence.

Moreover, the minimum losses are observed during the implementation of adaptive comb-filter based current control and voltage control techniques. The system structure for EVs charging is represented in figure 1, which consists of solar, battery and fuel cell sources. The incremental conductance based MPPT method is utilized and the seamless power transfer capability is achieved with the utilization of static transfer switches (STSs). The grid is utilized for power storage/transfer during the grid presence and with the grid-outage, the power is delivered to the local loads along with charging of EVs. Moreover, the maximum power is extracted from the proton exchange membrane (PEM) fuel cell stack through a maximum power tracking technique (MPPT), which is utilized for providing switching signal (Sfc) for the associated boost converter. In addition, battery energy storage (BES) is also utilized as a backup for emergency conditions. The common DC bus interconnection provides fast charging capability of EVs, along with the usage of a central inverter, which allows power transfer capability.

C. Structure of Control Technique

The charging of EVs is obtained here by the solar PV array, battery and fuel cell sources, along with improvement of power quality in accordance with the IEEE standards. The adaptive comb-filter control mechanism is utilized for generating the switching pulses of the inverter during grid interconnected mode of operation as shown in figure. Thus, uninterrupted power is provided to the local loads along with the charging of EVs during the grid connected mode of operation.

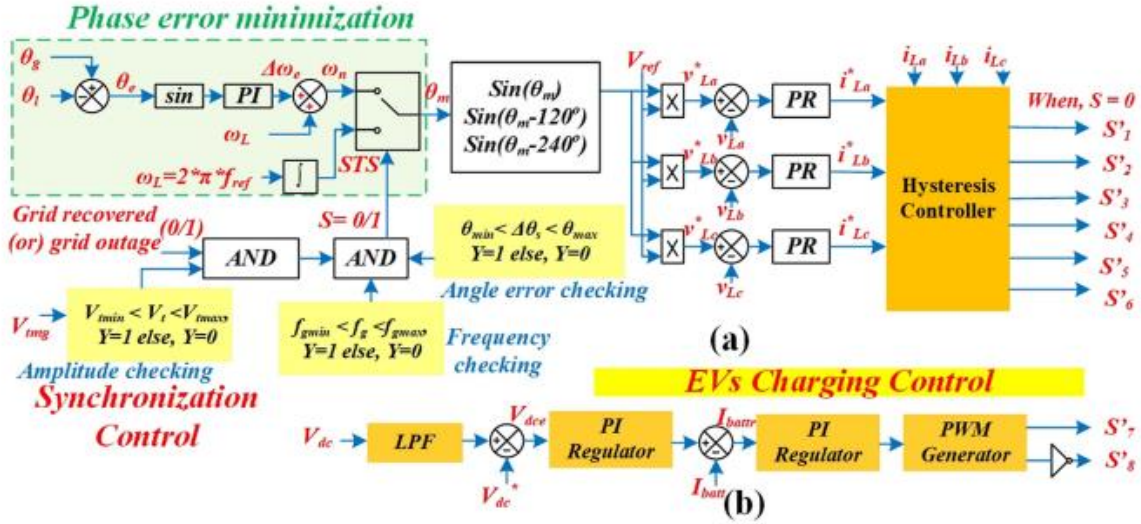

FIGURE 4. Control for operation during grid absence.

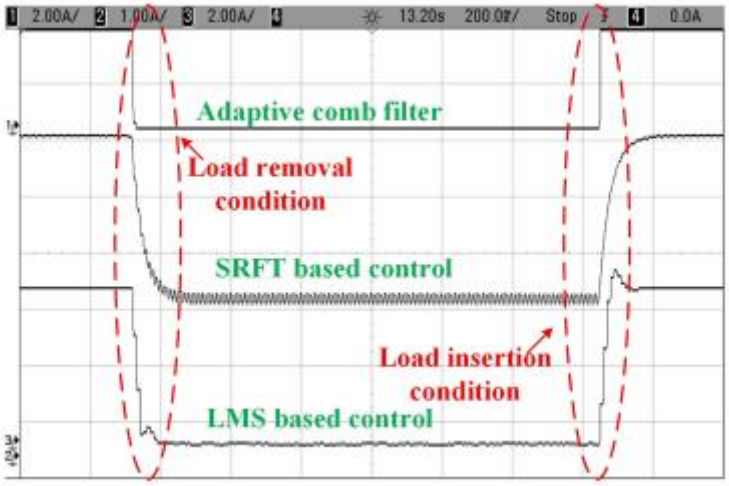

FIGURE 5. Comparative performance with respect to the weight convergence.

A Grid-Tied Mode of Operation for Common DC Bus EVs Charging System The grid line voltages (vsab, vsbc) are utilized to estimate the grid phase voltages as [16],

$$v_{sa} = \frac{v_{sbc}}{3} + \frac{2v_{sab}}{3}, v_{sb} = \frac{v_{sbc}}{3} - \frac{v_{sab}}{3},$$

$$v_{sc} = -\frac{2v_{sbc}}{3} - \frac{v_{sab}}{3}$$

Thus, by using obtained grid phase voltages (vsa, vsb, vsc), the terminal voltage (Vt) is evaluated as,

$$V_t = \sqrt{2(v_{sa}^2 + v_{sb}^2 + v_{sc}^2)/3}$$

The vsa, vsb, vsc and Vt are utilized to obtain upa, upb, upc and uqa, uqb, uqc as,

$$u_{pa} = v_{sa}/V_t, u_{pb} = v_{sb}/V_t, u_{pc} = v_{sc}/V_t$$

$$u_{qa} = \frac{-u_{pb}}{\sqrt{3}} + \frac{u_{pc}}{\sqrt{3}}, u_{qb} = \frac{3u_{pa}}{2\sqrt{3}} + \frac{u_{pb}}{2\sqrt{3}} - \frac{u_{pc}}{2\sqrt{3}}, u_{qc}$$

$$= \frac{-3u_{pa}}{2\sqrt{3}} + \frac{u_{pb}}{2\sqrt{3}} - \frac{u_{pc}}{2\sqrt{3}}$$

Moreover, the charging of EVs during the grid connected mode of operation, enables obtaining requisite energy from the grid for charging or returning the surplus renewable generation to the grid for storage purposes at an improved power quality. Thus, the charging of EVs is obtained using a cascaded PI constant current/ constant voltage controller for generating the switching pulses (S7 and S8) of the bidirectional converter as presented in Fig. 2(c). The sensed (Vev) and the reference voltages (V ∗ev) of EVs are utilized to obtain the voltage error (Veve) as,

$$\text{Veve} = \text{V} *\text{ev} - \text{Vev}$$

The output voltage error (Veve) obtained is utilized to obtain the reference current (I∗ev) of the EVs as follows,

$$\text{I}*\text{ev(m)} = \text{I}*\text{ev(m} - 1) + \text{Kpev } \{\text{Veve(m)}\} + \text{Kiev } \{\text{Veve(m)} - \text{Veve(m} - 1)\}$$

Furthermore, the current error Ieve is obtained as follows,

$$\text{Ieve} = \text{I}*\text{ev}–\text{Iev}$$

The current error (Ieve) obtained fed to a PI controller for generation of duty cycle for PWM switching pulses S7 and S8,

$$D_{eve}(m) = D_{eve}(m-1) + K_{peve}\{I_{eve}(m)\} + K_{ieve}\{I_{eve}(m) - I_{eve}(m-1)\}$$

Moreover, in order to enable the charging/discharging of the battery, the DC link voltage error is evaluated as,

$$\text{Vdce} = \text{V} * \text{dc} – \text{Vdc}$$

The estimated DC link voltage error obtained is utilized to obtain the reference battery current (I∗ batt) as follows,

$$I_{batt}^*(m) = I_{batt}^*(m-1) + K_{pdc}\{V_{dce}(m)\} + K_{idc}\{V_{dce}(m) - V_{dce}(m-1)\}$$

The I∗ batt is compared with the sensed battery current (Ibatt) as,

$$\text{Ibattr} = \text{I}* \text{ batt} –\text{Ibatt}$$

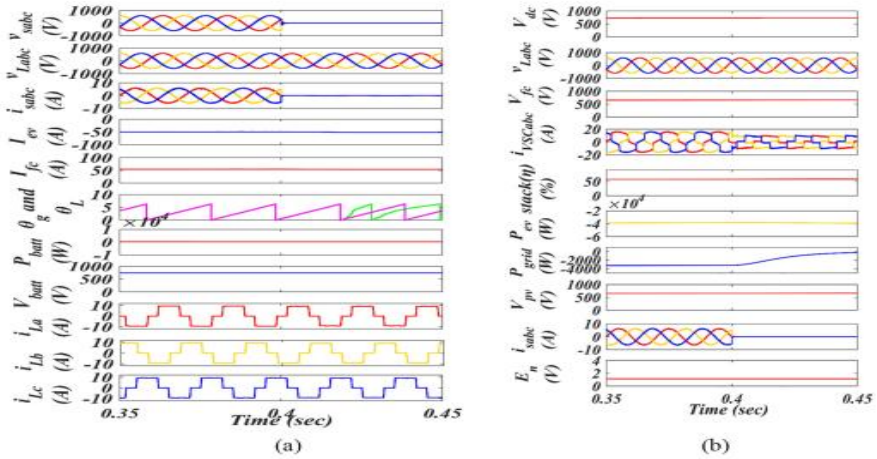

FIGURE 6. Mode change from grid-tied to standalone operation for common DC bus EVs charging system.

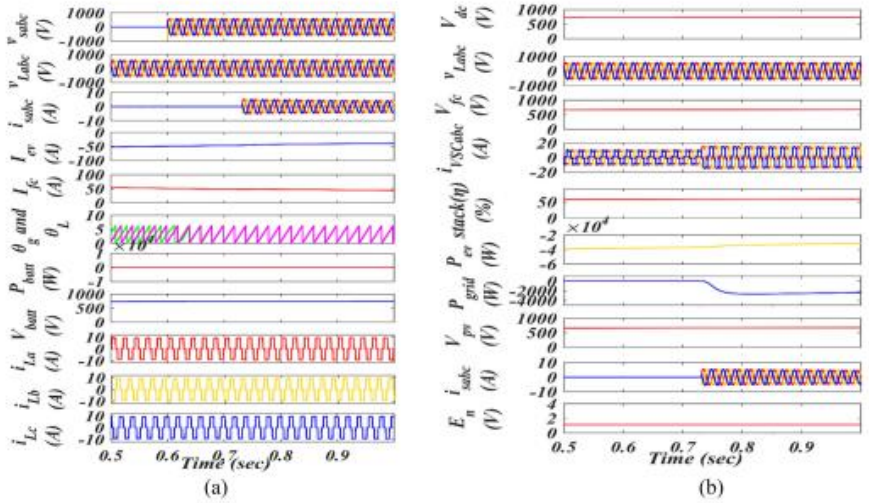

FIGURE 7. Mode change from standalone grid-tied to operation for common DC bus EVs charging system.

The obtained current error is given to the PI current controller to estimate the duty ratio for the bidirectional converter switching pulses S9-S10 in Fig. 2(e) as,

$$D(m) = D(m-1) + K_{pbatt}\{I_{battr}(m)\} + K_{ibatt}\{I_{battr}(m) - I_{battr}(m-1)\}$$

The advantages of utilizing a comb-filter, lie in its simple structure as its implementation utilizes only delays, adders and subtractions. Therefore, the adaptive comb-filter is utilized for obtaining the fundamental load current ifLa. The transfer function for estimating the fundamental of load current with the utilization of a comb-filter is given as,

$$\frac{i_{Lfa}}{i_{La}} = \frac{1}{M^2}\frac{\alpha(1-z^{-M})\delta(1-z^{M})}{(1-z^{-1})(1-z)}$$

Where, M = fs/fM, fs is the sampling frequency, fM is the fundamental of the periodic frequency and α, δ are the gains of the filter. Therefore, in order to set the gains of the filter with the existing cut-off frequency (ωc0) and the desired cut-off frequency (ωcα), the parameter α is obtained as [17]

$$\alpha = \left[\frac{\tan x}{\sin \omega_{c\alpha} + \tan x \cos \omega_{c\alpha}}\right], x = \frac{M\omega_{c0} - \omega_{c\alpha}}{2}$$

Thus, on further simplification, the transfer function obtained for the adaptive comb filter is given as follows,

$$\frac{i_{Lfa}}{i_{La}} = \frac{\alpha z^{-1}(\delta_1 + \gamma_1) - \left(\frac{\alpha(1-\gamma_1)}{z^{-1}}\right)\delta_1 - \left(\frac{\alpha(1-\delta_1)}{z^{-1}}\right)\gamma_1}{\delta_1\gamma_1}$$

Therefore, the fundamental component of the load current iLfa obtained is free from harmonics and sinusoidal in nature. The iLfa acquired is passed through zero crossing detector (ZCD), which is also provided with the quadrature phase unit templates (uqa, uqb, uqc). Consequently, after passing through the absolute block, load active power component (Ifpa) is obtained. Similarly,

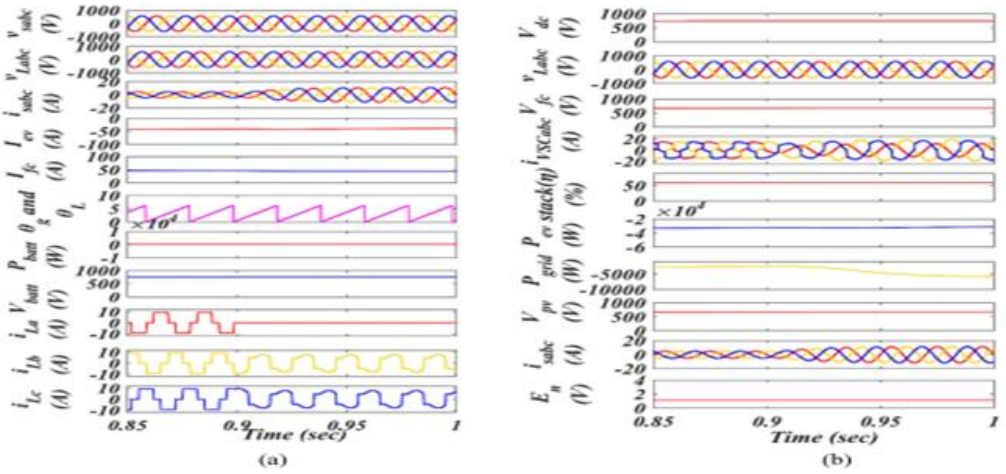

FIGURE 8. Performance of common DC bus EVs charging system during load unbalancing condition.

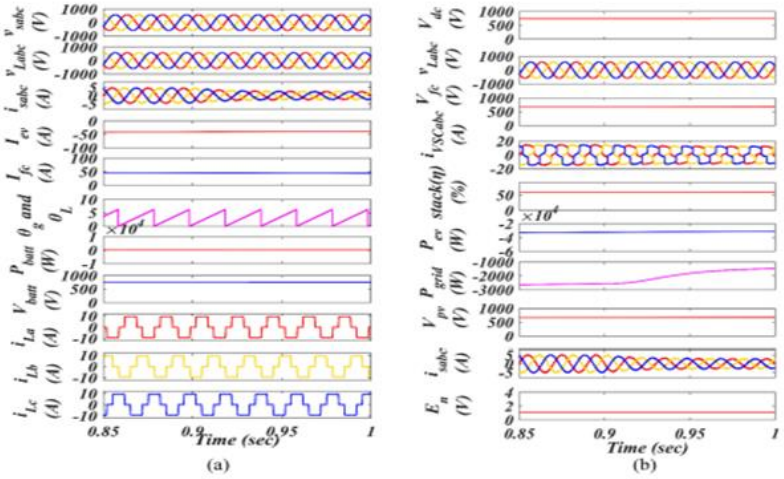

FIGURE 9. Performance of common DC bus EVs charging system during variable solar insolation condition.

Ifpb and Ifpc are determined and the average of load currents fundamental (Ifpa, Ifpb, Ifpc) component is estimated as,

IpLavg = (Ifpb + Ifpc + Ifpa)/3

Moreover, an INC based MPPT mechanism for maximum power extraction is utilized as presented in Fig. 2(d). The PV feed-forward wpv is calculated as,

$$wpv = (2Ppv)/(3Vt)$$

Furthermore, the control of the fuel cell is utilized through the efficient switching of (Sfc), which is obtained by PWM generator. The maximum power of the fuel cell is extracted through a MPPT technique as shown in Fig. 2(b) and the feed-forward term of the fuel cell, in order to improve the convergence rate is given as,

$$wf\,c = (2Pf\,c)/(3Vt)$$

Moreover, the contribution of the battery and EVs is given as,

$$wbatt = (2Pbatt)/(3Vt),\ wev = (2Pev)/(3Vt)$$

In order to obtain the grid active power component, the load active power component, PV feed-forward term, contribution of battery and fuel cell are utilized as,

$$Ipnet = IpLavg - (wpv + wf\,c + wbatt + wev)$$

The grid reference currents are evaluated by utilizing the grid active power component and the in-phase unit templates as,

$$i{*}sa = upa \times Ipnet,\ i{*}\,sb = upb \times Ipnet,\ i{*}sc = upc \times Ipnet$$

The current errors as obtained below are passed to the hysteresis controller for the generation of switching pulses S1-6 during grid connected mode of operation,

$$iesa = i{*}sa - isa,\ iesb = i{*}\,sb - isb,\ iesc = i{*}sc - isc$$

4. RESULTS AND DISCUSSION

Performance of common DC bus charging of EVs with distributed microgrid consisting of solar PV array, battery and fuel cell sources is presented here, where an adaptive comb-filter is utilized in order to improve the power quality during the grid connected mode of operation. The satisfactory performance is obtained during various conditions such as load removal, solar insolation reduction and grid outage conditions.

A. Mode Change between Grid

Connection to Disconnection for Common DC Bus EVs Charging System: The transition from grid connected to disconnected mode of operation for common DC bus charging of EVs with distributed microgrid consisting of solar PV array, battery and fuel cell sources. The grid voltages and grid currents are observed to reduce to zero at the instant of transition as presented in figure and power is delivered to the local loads along with charging of EVs. The fuel cell parameters are also presented such as fuel cell power (Pfc), voltage (Vfc) and the stack efficiency as shown in figure. In addition, the change in wave-shape of VSC currents is observed along with the grid power, which reduces to zero during the grid outage conditions.

B. Mode Change between Grid

Disconnection to Connection for Common DC Bus EVs Charging System: The mode change condition from grid disconnected to connected mode of operation is shown in figure. The matching of grid voltage and load voltage angles is observed along with the grid voltages and grid currents as presented in figure. Moreover, the figure shows the charging of EVs and iVSCabc, Vdc are also presented. The fuel cell provides power to the local loads and an increase is observed in the grid power at the instant of grid connected mode of operation.

C. Performance during Load Perturbation and Solar Radiation Variation

Performance during condition of load removal is presented in figure. The load of ‘a’ phase is removed and a subsequent

increase in the grid currents as shown in figure is observed due to the surplus power being fed to the grid. A change is observed in the load currents of remaining phases due to load removal condition and the battery power is observed constant due to the grid connected mode of operation. The figure shows the charging of EVs and an increase in grid power. In addition, the grid currents are observed to be sinusoidal and in agreement with an IEEE-519 standard. The figures present the solar insolation change condition and the decrease in grid currents due to the reduction in solar irradiation. The load currents, fuel cell current and the EV charging current are also presented. The load power is observed to be constant in magnitude along with grid and load voltages. Moreover, an increase is observed in the grid power during this condition as surplus power is fed to the grid. The power of EVs along with fuel cell stack efficiency, solar PV voltage and the DC link voltage are also presented in figures. EVs charging mechanism with hybrid renewable energy sources is obtained through the OPAL-RT controller (OP4510). Performances during grid connection/disconnection, load perturbation and solar radiation change are presented here and the results are recorded by using a digital storage oscilloscope.

D. EV Charging Capability under Conditions of Grid Presence/ Absence

The figures depict system behaviour during grid outage, where EVs are charged through coordinated control of the solar PV array and fuel cell. Grid voltage (vsa) drops to zero, and grid/load voltage angles lose synchronism, while load currents, battery voltage, and battery power remain constant. Fuel cell power, voltage, fuel flow rate, and stack efficiency are maintained during this period. Figures show the transition back to grid-connected mode, with voltage synchronization restored and EV charging current maintained. Grid current remains sinusoidal without harmonics, and line voltage with stack efficiency is preserved.

E. Variation in Charging of EVs under Conditions of Grid Presence/Absence

Performance during variation in charging of EVs during transition from grid connected to grid disconnected modes of operation is presented in figures. The grid voltage is reduced as observed in figure, along with an increase in battery charging current due to variation in power of EVs. Moreover, the decrease in grid power due to grid outage with battery power is observed in figure. In addition, the figures show the EV power change during the transition from grid disconnected to grid connected modes of operation, where the change in EV power is observed in figure with discharging of battery. Furthermore, the battery power, grid power and grid current are shown in figure, where the grid currents are observed at the instant of grid connection.

F. Performance under Weak Grid Conditions with Power Quality Improvement

Figures show that a reduction in solar insolation leads to decreased PV power and grid current, while fuel cell power compensates, and battery power/voltage remain unchanged. Figures depict load removal on phase ‘a’, causing unbalanced loading, reduced load power, and changes in VSC currents. Surplus power is fed to the grid, increasing grid current magnitude along with EV charging power. Battery parameters remain constant during these disturbances. Figures show that applying an adaptive comb-filter reduces grid current THD to 1.57% from 24.89% in load current, with load voltage THD at 2.159%, improving power quality. In standalone mode, load current THD is 24% and load voltage THD is 1.89% as shown in figures.

5. CONCLUSION AND FUTURE SCOPE

Performance of common DC bus EV charging infrastructure has been demonstrated with DERs consisting of solar, battery and fuel cell sources. The hybrid system is preferred due to the reduced effect of inconsistency often observed during utilization of renewable sources. Moreover, with the usage of common DC bus charging infrastructure for EVs, fast charging of EVs is obtained as the on-board charger of EVs is bypassed, thereby, delivering direct power to the EV battery. Thus, the charging ability is not limited by the power of the on-board charger. In addition, the power quality of the system is also improved with the usage of adaptive comb-filter based control techniques during grid interconnection and standalone mode, a voltage control is employed. Therefore, satisfactory performance of system has been observed for various scenarios like grid connection/disconnection, load perturbation and solar radiation change and validated through test results in accordance with the IEEE standards.

REFERENCES

[1]. C. Gonçalves, P. Pinson, and R. J. Bessa, "Towards data markets in renewable energy forecasting," IEEE Trans. Sustain. Energy, vol. 12, no. 1, pp. 533–542, Jan. 2021.

[2]. X. Yang, Y. Zhang, F. Zhang, C. Xu, and B. Yi, "Enhancing utilization of PV energy in building microgrids via autonomous demand response," IEEE Access, vol. 9, pp. 23554–23564, 2021.

[3]. R.-J. Wai and W.-H. Wang, "Grid-connected photovoltaic generation system," IEEE Trans. Circuits Syst., vol. 55, no. 3, pp. 953–964, Apr. 2008.

[4]. S. Jain, J. Jiang, X. Huang, and S. Stevandic, "Modeling of fuel-cell-based power supply system for grid interface," in Proc. IEEE Joint Int. Conf. Power Syst. Technol. Power India Conf., 2008, pp. 1–8.

[5]. F. Ahmad, M. S. Alam, S. M. Shariff, and M. Krishnamurthy, "A costefficient approach to EV charging station integrated community microgrid: A case study of Indian power market," IEEE Trans. Transp. Electrific., vol. 5, no. 1, pp. 200–214, Mar. 2019.

[6]. M. Patterson, N. F. Macia, and A. M. Kannan, "Hybrid microgrid model based on solar photovoltaic battery fuel cell system for intermittent load applications," IEEE Trans. Energy Conv., vol. 30, no. 1, pp. 359–366, Mar. 2015.

[7]. M. S. Islam, N. Mithulananthan, and K. Y. Lee, "Suitability of PV and battery storage in EV charging at business premises," IEEE Trans. Power Syst., vol. 33, no. 4, pp. 4382–4396, Jul. 2018.

[8]. A. Khan, S. Memon, and T. P. Sattar, "Analyzing integrated renewable energy and smart-grid systems to improve voltage quality and harmonic distortion losses at electric-vehicle charging stations," IEEE Access, vol. 6, pp. 26404–26415, 2018.

[9]. V.Monteiro, J. G. Pinto, and J. L. Afonso, "Operation modes for the electric vehicle in smart grids and smart homes: Present and proposed modes," IEEE Trans. Veh. Technol., vol. 65, no. 3, pp. 1007–1020, Mar. 2016.

[10]. G. Zhu, Q. Yuan, and X. Yang, "Research and analysis of SOGI-QSG integral saturation in the application of grid synchronization," in Proc. IEEE Int. Conf. Mech. Automat., 2019, pp. 1167–1171.

[11]. J. Ospina et al., "Sampling-based model predictive control of PV-integrated energy storage system considering power generation forecast and realtime price," IEEE Power Energy Tech. Syst. J., vol. 6, no. 4, pp. 195–207, Dec. 2019.

[12]. H. M. M. Alhaj, N. M. Nor, V. S. Asirvadam, and M. F. Abdullah, "Power system harmonics estimation using LMS, LMF and LMS/LMF," in Proc. IEEE Int. Conf. Intell. Adv. Syst., 2014, pp. 1–5.

[13]. P. Shukl and B. Singh, "Distributed energy resources-based EV charging station with seamless connection to grid," in Proc. IEEE Int. Conf. Comp. Commun. Automat., 2021, pp. 57–62.

[14]. IEEE Recommended Practice for Interconnecting Distributed Resources with Electric Power Systems Distribution Secondary Networks, IEEE Standard 1547, 2014.

[15]. IEEE Recommended Practices and Requirements for Harmonic Control on Electric Power System, IEEE Standard 519, 2014.